Magnetization and spin diffusion of liquid ³He in aerogel

J. A. Sauls,[1,2] Yu. M. Bunkov,[1] E. Collin,[1] H. Godfrin,[1] and P. Sharma[2]

[1]*Centre de Recherches sur les Très Basses Températures, Centre National de la Recherche Scientifique,
Laboratoire Associé à l'Université J. Fourier, Boîte Postale 166, 38042 Grenoble Cedex 9, France*
[2]*Department of Physics & Astronomy, Northwestern University, Evanston, Illinois 60208, USA*

We report theoretical calculations and experimental measurements of the normal-state spin diffusion coefficient of ³He in aerogel, including both elastic and inelastic scattering of ³He quasiparticles, and compare these results with data for ³He in 98% porous silica aerogel. This analysis provides a determination of the elastic mean free path within the aerogel. Measurements of the magnetization of the superfluid phase in the same aerogel samples provide a test of the theory of pairbreaking and magnetic response of low-energy excitations in the "dirty" B phase of ³He in aerogel. A consistent interpretation of the data for the spin-diffusion coefficient, magnetization, and superfluid transition temperature is obtained by including correlation effects in the aerogel density.

I. INTRODUCTION

A strongly correlated Fermi liquid in the presence of disorder is realized when ³He is introduced into highly porous silica aerogel. The effects of disorder on the phase diagram and low-temperature properties of superfluid ³He have been a subject of widespread current interest. The thermodynamic and transport properties of ³He in aerogel are strongly modified by the scattering of ³He quasiparticles off the low-density aerogel structure. Here we summarize theoretical calculations of the magnetization[1] and spin transport[2] in the normal and superfluid states of ³He in high-porosity aerogel. The theoretical results are compared with experimental measurements of the normal-state spin-diffusion coefficient and magnetic susceptibility of the superfluid phase over the temperature range 1 mK ≲ T ≲ 100 mK.[3]

For 98% porosity the typical diameter of the silica strands is $\delta \simeq 3$ nm. The mean distance between strands is $\xi_a \simeq 40$ nm, which is large compared to the Fermi wavelength, $\lambda_f \sim 0.1$ nm, but comparable to or less than the bulk coherence length, $\xi_0 = \hbar v_f / 2\pi T_{c0} \simeq 20-80$ nm over the pressure range $p = 34-0$ bar. The aerogel does not modify the bulk properties of normal ³He, beyond the formation of a couple of atomic layers of solid-like ³He adsorbed on the silica strands. The main effect of the aerogel structure is to scatter ³He quasiparticles moving with the Fermi velocity. At temperatures below $T^* \approx 10$ mK elastic scattering by the aerogel dominates inelastic quasiparticle-quasiparticle collisions.[4] This limits the mean free path of normal ³He quasiparticles to $l \simeq 130-180$ nm for aerogels with 98% porosity. (Note that there are variations in mean free path and correlation length for different aerogels with the same porosity.) Thus, the low-temperature limit for the spin diffusion coefficient is determined by elastic scattering from the aerogel. Comparison with experimental measurements for $T \ll T^*$ provides a determination of the transport mean free path due to scattering of quasiparticles by the aerogel.

Scattering by the aerogel also has dramatic effects on the formation and properties of the superfluid phases. If the coherence length (pair size) is sufficiently long compared to the typical distance between scattering centers, then the aerogel is well described by a homogeneous, isotropic scattering medium (HSM) with a mean-free path determined by the aerogel density. However, more elaborate scattering models are required if aerogel density correlations develop on length scales that are comparable with the pair correlation length.[5] Density correlations are observed at wave vectors $q \gtrsim \pi/\xi_a$ in the aerogel structure factor. We identify ξ_a with the typical distance between silica strands or clusters, $\xi_a \approx 30-50$ nm (c.f. Fig. 1). Figure 2 shows a comparison of the pair correlation length (Cooper pair size), $\xi = \hbar v_f / 2\pi T_c$, as a function of pressure for ³He in aerogel, as well as that for pure ³He ($\xi_0 = \hbar v_f / 2\pi T_{c0}$), with an aerogel correlation length of $\xi_a = 40$ nm.

The HSM provides a reasonable approximation to the properties of superfluid ³He-aerogel at low pressures; this model accounts semiquantitatively for the reduction of T_c, including the critical pressure p_c and the pair-breaking suppression of the order parameter.[4,5] However, the HSM becomes a poorer description of ³He-aerogel at higher porosities and higher pressures where the pair size is comparable to, or smaller than, the typical distance between scattering centers. This breakdown of the HSM is first evident in the quantitative discrepancies in the pressure dependence of T_c, particularly for higher porosity aerogels.[5,6]

The inhomogeneity of the aerogel on scales $\xi_a \gtrsim \xi$ leads to higher superfluid transition temperatures than predicted by the HSM with the same quasiparticle mean free path. Regions of lower aerogel density, of size of order ξ_a, are available for formation of the condensate. Thus, the qualitative picture is that of a random distribution of low density regions, "voids," with a typical length scale ξ_a in an aerogel with a quasiparticle mean-free path l. In the limit $\xi \sim \xi_a \ll l$, the superfluid transition is determined by the pairbreaking effects of dense regions surrounding the "voids," and scales as $\delta T_c/T_{c0} \propto -(\xi/\xi_a)^2$. However, when the pair size is much larger than ξ_a the aerogel is effectively homogeneous on the scale of the pairs and pairbreaking results from homoge-
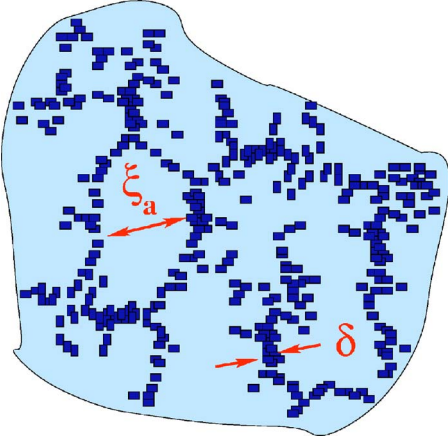
FIG. 1. (Color online) A model silica aerogel showing low-density regions (light) of ^{3}He surrounded by higher density strands and aggregates of silica (dark). The aerogel correlation length, $\xi_a \approx 40$ nm, is identified with the mean interstrand distance. The aerogel strand diameter is approximately, $\delta \simeq 3$ nm.

neous scattering defined by the transport mean free path, which scales as $\delta T_c/T_{c0} \propto -(\xi/l)$. This latter limit is achieved at low pressures. Here we adopt a simplified version of the inhomogeneous scattering model[5] that incorporates correlations of the aerogel. The correlation effect is included by introducing an effective pairbreaking parameter that interpolates between these two limits: $x \to \tilde{x} = x/(1+\zeta_a^2/x)$, where $x = \xi/l$ and $\zeta_a \equiv \xi_a/l$. This heuristic treatment of aerogel correlations provides a good description of the pressure dependence of T_c in zero field for ^{3}He in aerogel over the whole pressure range.[7]

In Sec. II we summarize experimental results for the magnetization of normal ^{3}He in aerogel, which are used to determine the amount and effect of the solid-like component of ^{3}He that coats the aerogel strands. Section III describes nuclear magnetic resonance (NMR) measurements of the spin diffusion coefficient of normal liquid ^{3}He in aerogel and the theoretical calculations used to determine the elastic mean free path of quasiparticles. In p-wave superfluids quasiparticle scattering from the aerogel medium is intrinsically pairbreaking and leads to renormalization of nearly all properties of the superfluid phases. In Sec. IV we summarize an analysis of the effects of scattering by the aerogel on the magnetic susceptibility based on the theoretical results for the disordered Balian-Werthamer (BW) phase,[1] modified to include the reduced pair-breaking effect of low-density regions of aerogel. The "dirty" B phase is believed to describe the zero-field phase of superfluid ^{3}He in aerogel, except in a narrow region near T_c.[8] The theory for the magnetization based on the "dirty" B phase is tested against the measurements of the susceptibility.[3]

II. MAGNETIZATION OF NORMAL ^{3}He

The nuclear magnetization M of normal liquid ^{3}He at temperatures $k_B T \ll E_f$ and fields $\gamma \hbar H \ll E_f$ is given in terms of the (single-spin) quasiparticle density of states at the Fermi level N_f, the nuclear gyromagnetic ratio for ^{3}He γ, and
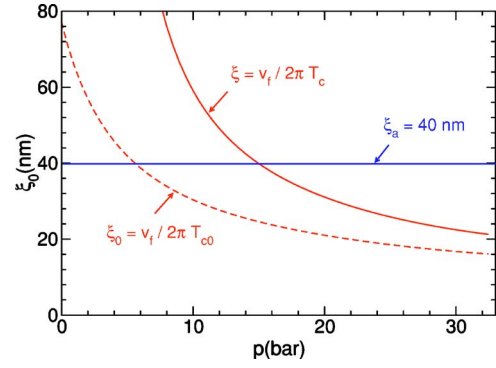

FIG. 2. (Color online) The pair correlation length of superfluid ^{3}He in aerogel (solid curve) as a function of pressure is shown in comparison with an aerogel strand-strand correlation length $\xi_a \simeq 40$ nm. A crossover occurs near $p \approx 15$ bar. The bulk ^{3}He correlation length is also shown (dashed curve).

the exchange enhancement of the local field given in terms of the Landau interaction parameter F_0^a, $\chi_N = M/H = 2N_f\mu^2/(1+F_0^a)$, where $\mu = \gamma\hbar/2$ is the nuclear magnetic moment of the ^{3}He nucleus; χ_N is the nuclear spin susceptibility of the normal Fermi liquid.

The effect of the aerogel on the magnetization of the normal liquid phase of ^{3}He is expected to be negligible. However, the aerogel structure is known to be covered with one or two layers of localized ^{3}He atoms. These surface layers contribute a Curie-like susceptibility that obscures the Fermi-liquid contribution at low temperatures.[9] The surface contribution can be suppressed by the addition of ^{4}He which preferentially plates the aerogel structure. The net effect is twofold: (1) the surface Curie susceptibility is suppressed and (2) spin-spin scattering between ^{3}He quasiparticles and the surface spins is suppressed. The cross section of the aerogel may also be modified by ^{4}He preplating, but we expect this effect to be relatively small.

We have performed accurate measurements of the magnetic susceptibility of normal liquid ^{3}He in aerogel, with and without ^{4}He preplating, using continuous wave (cw) NMR at a field of $H = 37.3$ mT over a wide range of pressures and temperatures from $T \simeq 1$ mK up to a few hundred mK. The temperature was measured using the vibrating wire technique described in Ref. 10. The high-temperature regime was calibrated against the Fermi temperature T_F and the melting curve thermometer. In Fig. 3 we show the magnetization data as a function of temperature for several pressures. The data are fit to a two-component form for the susceptibility; a Curie-Weiss term to describe the solid susceptibility with ferromagnetic correlations plus a temperature-independent term for the bulk Fermi liquid $\chi = C/(T-\Theta_w) + \chi_N$. The fit allows us to determine the ratio of the number of solid to liquid ^{3}He atoms as a function of pressure, as well as the Curie-Weiss temperature of the solid spins. Pressurizing ^{3}He in aerogel leads to increased solidification of ^{3}He atoms, as shown in Fig. 4 and a decrease in the Curie-Weiss temperature as shown in Fig. 5. Both effects are well understood from previous studies on ^{3}He adsorbed on homogeneous substrates (e.g., graphite) or heterogeneous substrates (powders, Vycor, etc.).[11,12] These results allow us to remove the
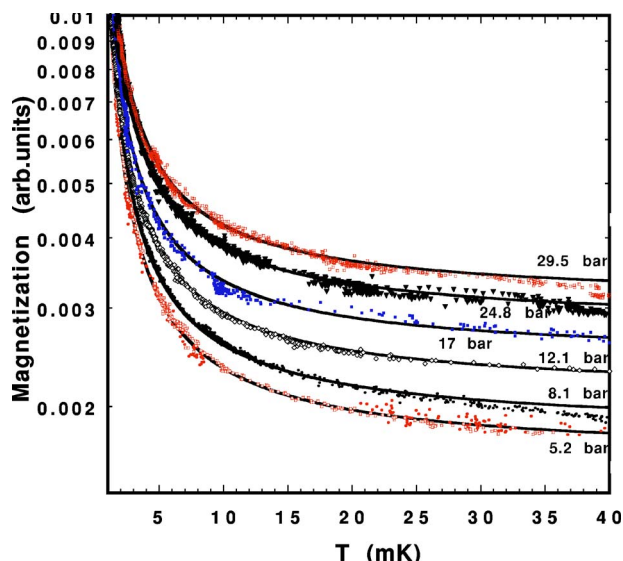
FIG. 3. (Color online) The total magnetization of ^{3}He in aerogel, both liquid and solid, for several pressures.

contribution to the susceptibility from solid ^{3}He, and thus to extract the susceptibility of liquid ^{3}He below superfluid transition.

We also performed measurements of the susceptibility of ^{3}He in aerogel by preplating with ^{4}He atoms. We added a small amount of ^{4}He at a temperature of about 3 K and then cooled it down. The solid ^{3}He susceptibility is used to measure the amount of ^{4}He adsorbed on the aerogel strands. The Curie-Weiss temperature is found to decrease in proportion to the amount of residual solid ^{3}He.

For the NMR experiments reported here the solid and liquid components of ^{3}He in aerogel exhibit a common NMR line, and are in the limit of "fast exchange" with a resonance
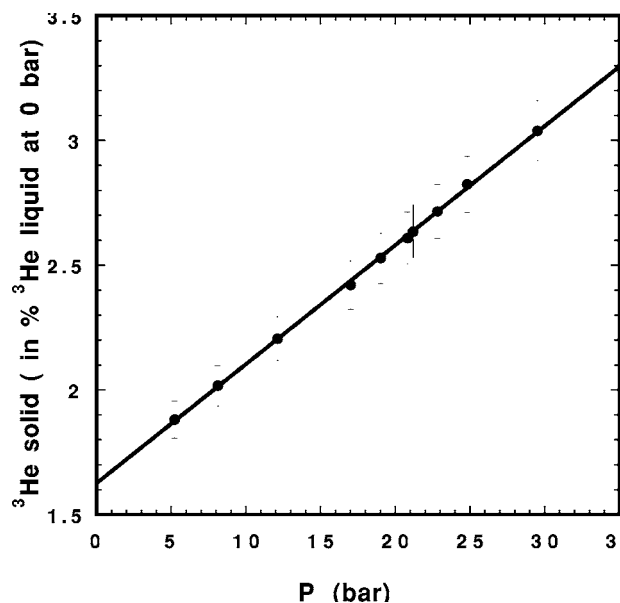

FIG. 4. The density of solid ^{3}He atoms, normalized by density of liquid ^{3}He for $p=0$ bar.
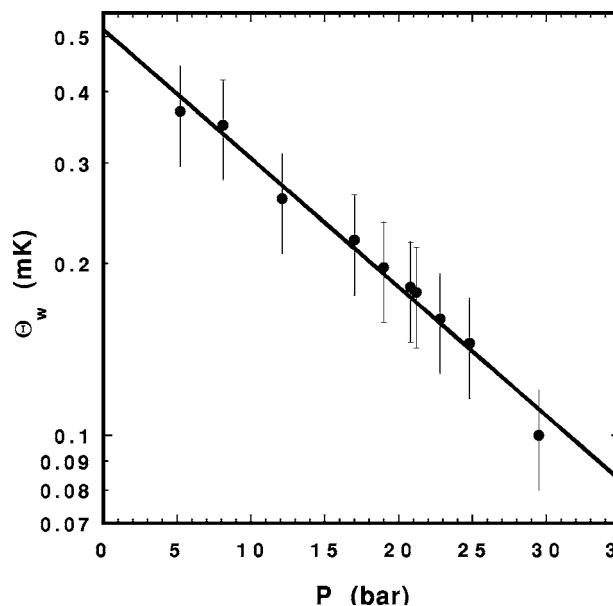

FIG. 5. The Curie-Weiss temperature, Θ_W, as a function of pressure. The decrease reflects the increased average density of the solid layer in equilibrium with liquid ^{3}He as the pressure increases.

frequency determined by the weighted average of the liquid and solid resonance frequencies, $\langle\omega\rangle=(M_{\text{liquid}}\omega_{\text{liquid}}+M_{\text{solid}}\omega_{\text{solid}})/(M_{\text{liquid}}+M_{\text{solid}})$.[9] We have performed the measurement of first and second moments of the NMR line, with and without ^{4}He preplating. The NMR line is broadened by the presence of solid ^{3}He by as much as 12 μT, and the broadening scales by the ratio of the solid to liquid magnetization.

These experiments combined with NMR measurements of the spin-diffusion process in a field gradient provide a detailed characterization of the magnetic properties of solid and liquid ^{3}He in the aerogel sample. The determination of the solid ^{3}He magnetization, and the extrapolation of the Curie-Weiss behavior to temperatures below the superfluid transition, allow us to extract the liquid component of the susceptibility in the superfluid phase of ^{3}He in aerogel. Measurements of the spin-diffusion coefficient in the normal phase of ^{3}He provide a measurement of the transport mean free path in aerogel.

III. SPIN DIFFUSION

Measurements of the spin-diffusion coefficient for ^{3}He in 98% aerogel were performed with small amounts of ^{4}He added in order to displace the solid ^{3}He. At $p=0$ bar we see no signature of solid ^{3}He, while at $p=29.5$ bar we observe a small fraction ($\approx 0.25\%$ in the units of Fig. 4) of solid ^{3}He.

We have used the typical spin echo sequences, $\pi/2-\tau-\pi$ and $\pi/2-\tau-\pi/2$, to measure the decay of echo signal as a function of time delay τ at a magnetic field gradient $G_z=23$ μT/cm. The solution of the Bloch equations for the spin echo signal in the magnetic field gradient reads is given by $H=H_0\exp(-2\tau/T_2-A\tau^3)$, where $A=\frac{2}{3}D_M(\gamma G_z)^2$. The decay of the spin echo is shown in Fig. 6 as function of
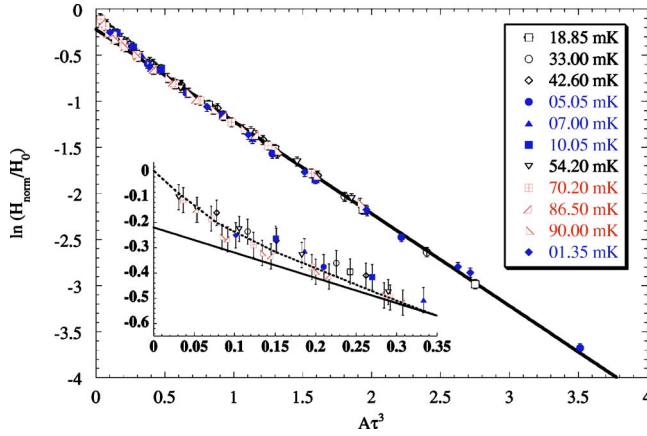
FIG. 6. (Color online) The τ^3 decay of the echo signal in a magnetic field gradient for $p=0.5$ bar. The temperature range is from $T=1$ to 90 mK. The coefficient A, determined from the fit at a fixed temperature, is related to the spin-diffusion coefficient and field gradient. The inset shows the short time, fast relaxation of unknown origin.

$A\tau^3$ for our experimental conditions. On short time scales we observe small deviations from the τ^3 dependence. These deviations are indicative of a fast relaxation mechanism of unknown origin. However, the main feature of the data is the τ^3 dependence due to spin diffusion in a magnetic field gradient. The echo decay thus provides a direct measure of the spin diffusion coefficient of ^{3}He in aerogel.

In pure ^{3}He, the transport of magnetization in the hydrodynamic limit is given by the magnetization current density,

$$\mathbf{j}_i = -D_M \boldsymbol{\nabla} M_i, \tag{1}$$

where M_i is the ith component of the local magnetization, $\mathbf{M}(\mathbf{r},t)$, and D_M is the spin diffusion coefficient. The hydrodynamic coefficient can be calculated from a kinetic theory of quasiparticles, which in the case of ^{3}He in aerogel is the Landau-Boltzmann transport equation with the collision integral determined by both elastic scattering from the aerogel medium and inelastic quasiparticle collisions, i.e., binary collisions of quasiparticles within the narrow energy shell of order $k_B T$ near the Fermi surface. The general solution has the form

$$D_M = \tfrac{1}{3} v_f^2 (1 + F_0^a) \tau_{\mathrm{D}}, \tag{2}$$

in the hydrodynamic limit, $\omega_{\mathrm{L}} \ll \tau_{\mathrm{D}}^{-1}$, where $\omega_{\mathrm{L}} = \gamma H$ is the Larmor frequency, τ_{D}^{-1} is the collision rate that limits the transport of magnetization, v_f is the Fermi velocity, and F_0^a is the $l=0$ exchange interaction for ^{3}He quasiparticles. The collision rate is calculated from the solution of the Landau-Boltzmann transport equation including both scattering channels.[13] The result of this calculation is summarized below.

At high temperatures $(T \gg T^*)$ inelastic binary collisions of the quasiparticle limit the transport of spin. The diffusion time approaches the bulk transport time[15]

$$\tau_{\mathrm{D}} \to \tau_{\mathrm{D}}^{\mathrm{bulk}} = \frac{2\tau_{\mathrm{in}}}{\pi^2} \sum_{\nu=1}^{\mathrm{odd}} \frac{(2\nu+1)}{\nu(\nu+1)[\nu(\nu+1)-2\lambda_D]}, \tag{3}$$

where the inelastic quasiparticle lifetime is given by

$$\tau_{\mathrm{in}}^{-1} = \frac{N_f^2}{2p_f v_f} \langle W \rangle T^2, \tag{4}$$

with N_f the single-spin density of states at the Fermi energy, and W the binary collision probability for quasiparticles on the Fermi surface with momenta $|\mathbf{p}_i| = p_f$. The Fermi-surface average is defined by

$$\langle W \rangle = \int \frac{d\Omega}{4\pi} \frac{W(\theta,\phi)}{2\cos(\theta/2)}, \tag{5}$$

where $W(\theta,\phi)$ is the scattering probability for binary collisions of quasiparticles on the Fermi surface, defined in terms of the standard scattering angles. The parameter λ_D is given by the following average of the spin-flip scattering rate[16]

$$\lambda_D = 1 - \frac{1}{\langle W \rangle} \int \frac{d\Omega}{4\pi} \frac{W_{\uparrow\downarrow}(1-\cos\theta)(1-\cos\phi)}{4\cos(\theta/2)}. \tag{6}$$

However, at sufficiently low temperatures the scattering rate is limited by the quasiparticle collisions with the aerogel medium. Hence, as the temperature is reduced, the diffusion coefficient crosses over from a clean-limit behavior, $D_M \propto T^{-2}$, to an impurity-dominated regime in which the diffusion coefficient approaches a temperature-independent value given by

$$\tau_{\mathrm{D}} \to \tau_{\mathrm{el}} = l/v_f, \quad T \ll T^*, \tag{7}$$

where l is the limiting mean-free path for quasiparticles propagating ballistically through ^{3}He then scattering elastically off the aerogel structure. This is the geometric mean free path for classical (point) particles, i.e., quasiparticles traveling through the aerogel medium. Note that in the limit $T \ll T^*$ Eq. (7) for τ_{D} is exact for nonmagnetic elastic scattering by the aerogel.[14]

At intermediate temperatures the temperature dependence of the diffusion time is determined by both scattering channels; the result for τ_{D} is given in the Appendix, and the calculated spin diffusion coefficient is shown in Fig. 7 for $p=0.5$ bar and for $p=29.5$ bar. The spin-diffusion coefficient decreases as $D_M \propto T^{-2}$ at high temperatures and coincides with the bulk measurements of the ^{3}He spin-diffusion coefficient by Ref. 18. Thus, we fit the average binary quasiparticle collision probability $\langle W \rangle$ at each pressure to the high-temperature diffusion coefficient with the spin-flip scattering rate parameter λ_{D} obtained from the scattering model of Ref. 19. The bulk Fermi liquid parameters used in the calculation of D_M for ^{3}He in aerogel are taken from Ref. 20.

The low-pressure results provide the best data set to compare with the theory. The theoretical result shown in Fig. 7 corresponds to a low-temperature (elastic) mean free path of $l=130$ nm. Note that the crossover from the high-temperature inelastic limit to the low-temperature aerogel-dominated regime is well described by the theory at low pressure.
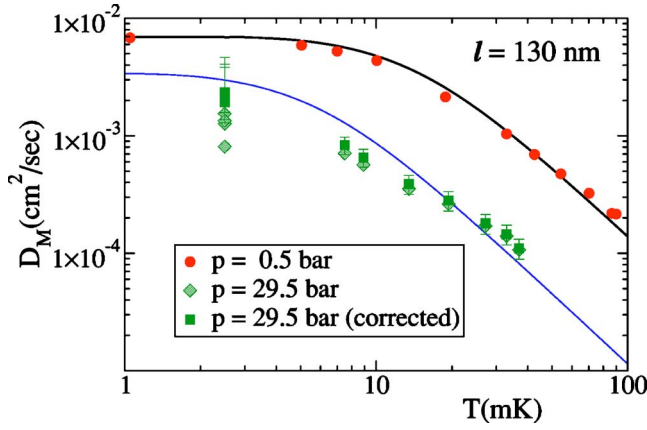
FIG. 7. (Color online) Comparison to our experimental data (see Ref. 3). We fit the inelastic scattering amplitude to the high-temperature data and obtain good agreement for a mean free path $l=130$ nm for the entire temperature range.

The aerogel mean-free path is expected to be essentially pressure independent, as long as the integrity of the aerogel is not damaged under hydrostatic pressure. Thus, the calculation of the spin-diffusion coefficient is made with the same aerogel mean-free path and the bulk scattering parameters appropriate for $p=29.5$ bar. The result is also shown in Fig. 7. The experimental data are consistent with the theoretical results within the estimated errors. The higher pressure spin-diffusion data are also shown corrected for the small, but measurable, component of solid magnetization that is transported by diffusion due to fast exchange with the liquid. The main result of this analysis is the determination of the elastic mean free path. This parameter is relevant to the mechanism for pair breaking, the low-energy excitation spectrum, and polarizability of the superfluid phase of ^{3}He in aerogel.

Measurements of the spin diffusion coefficient for ^{3}He in denser aerogel (porosity $P=95\%$) are reported in Ref. 21. These authors observed the crossover to the low-temperature regime dominated by elastic scattering from the aerogel strands. Their measurement of the low-temperature limit of the diffusion constant corresponds to an aerogel mean-free path of $l=58$ nm. This result is in close agreement with theoretical expectations for the mean-free path for this density and our result of $l=130$ nm obtained for 98% aerogel. Specifically, the geometric mean-free paths for two aerogels $l_{1,2}$ formed from silica strands of the same typical diameter can be shown to scale inversely with their respective volume fractions, i.e., $l_1=l_2(\varrho_2/\varrho_1)$, where $\varrho=1-P$. Thus, based a mean-free path of $l_2=130$ nm for $1-\varrho_2=98\%$ we expect a mean-free path of $l_1=52$ nm for $1-\varrho_1=95\%$ aerogel, which is close to that reported by Ref. 21.

IV. MAGNETIZATION OF ^{3}He-B-AEROGEL

Measurements of the B-like suppression of the susceptibility in ^{3}He-aerogel have been reported for two or more monolayers of ^{4}He added to displace the solid layer of ^{3}He.[9,22] Experiments carried out in Grenoble[3] on pure ^{3}He in

aerogel also show the B-like suppression of the liquid component of the susceptibility, obtained by subtracting the Curie-Weiss component from the solid ^{3}He coating the aerogel strands. In the following section we compare theoretical results for the magnetic susceptibility of the "dirty B phase" of superfluid ^{3}He with these recent experimental measurements. The magnetization measurements in the superfluid phase were carried out on the same aerogel used in measurements of the spin echo decay. Thus, the transport mean-free path of this aerogel, $l=130$ nm, is known.

In the theoretical analysis of the magnetization we consider only elastic scattering of ^{3}He quasiparticles off the aerogel structure, and we neglect the spin dependence of the scattering cross section for ^{3}He quasiparticles by the polarized solid. The splitting of the cross section by the polarized solid is expected to be a very small effect which is unimportant in calculating pair-breaking effects, except in a very narrow temperature interval corresponding to the A_1-A_2 transition.[7]

The nuclear spin susceptibility of pure superfluid ^{3}He-B agrees quantitatively to leading order in T_c/E_f with the result of Ref. 23 for the susceptibility of the Balian-Werthamer state

$$\chi_B/\chi_N = \frac{(1+F_0^a)\left[\frac{2}{3}+Y\left(\frac{1}{3}+\frac{1}{5}F_2^a\right)\right]}{1+F_0^a\left(\frac{2}{3}+\frac{1}{3}Y\right)+\frac{1}{5}F_2^a\left(\frac{1}{3}+\frac{2}{3}Y\right)+\frac{1}{5}F_2^a F_0^a Y}, \quad (8)$$

where $Y(T)$ is the well-known Yosida function

$$Y(T) = 1 - \pi T \sum_{\varepsilon_n} \frac{\Delta^2}{[\varepsilon_n^2+\Delta^2]^{3/2}}, \quad (9)$$

$\Delta(T)$ is the B-phase gap amplitude, and F_2^a is the $l=2$ harmonic of the exchange interaction.

For a B-like phase of ^{3}He in aerogel depairing of the $S_z=0$ Cooper pairs by scattering from the aerogel leads to sizable changes in the magnetization. In addition to the suppression of T_c relative to T_{c0}, the magnitude of the susceptibility, particularly at low temperatures, is sensitive to the density of quasiparticle states below the gap, $\varepsilon < \Delta$, produced by pair breaking.

In the HSM model, for either Born or unitarity scattering, the generic form of Eq. (8) for the B-phase susceptibility is preserved with the replacement of the gap and Yosida functions by impurity-renormalized gap and response functions.[1,24] The results can be summarized by Eq. (8) with the replacement of $Y(T) \rightarrow \widetilde{Y}(T)$. For example, in the unitary scattering limit

$$\widetilde{Y} = 1 - \pi T \sum_n \frac{\Delta^2}{[\widetilde{\varepsilon}_n^2+\Delta^2]^{3/2}} \left\{ \frac{1}{1+\frac{1}{3}\left(\frac{1}{\widetilde{\varepsilon}_n}\right)^2 \frac{\Gamma_N \Delta^2}{\sqrt{\widetilde{\varepsilon}_n^2+\Delta^2}}} \right\}, \quad (10)$$

where Γ_N is related to the aerogel mean-free path for normal-state ^{3}He quasiparticles
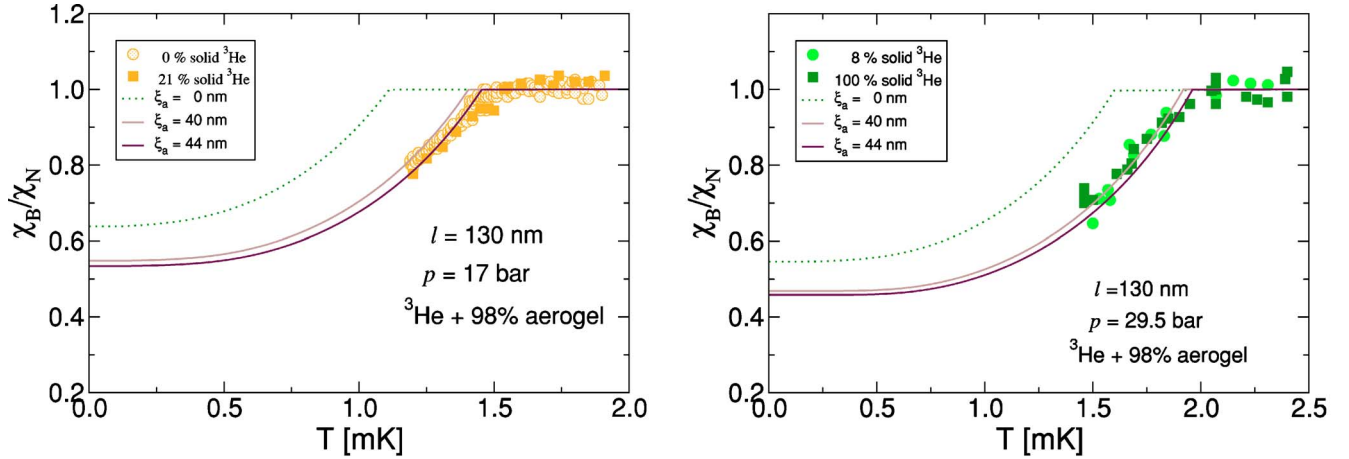
FIG. 8. (Color online) Comparison to experimental data for the magnetic susceptibility at $p=17$ bar and $p=29.5$ bar. Only the liquid contribution to the susceptibility is plotted for the measurements with different amounts of solid ^{3}He. The theoretical calculations are based on the HSM and the dirty BW phase.

$$\Gamma_N = \frac{\hbar v_f}{2l}. \tag{11}$$

The gap equation and renormalized Matsubara frequencies are given by

$$\ln(T/T_{c0}) = \pi T \sum_n \left(\frac{1}{\sqrt{\tilde{\varepsilon}_n^2 + \Delta^2}} - \frac{1}{|\varepsilon_n|} \right), \tag{12}$$

$$\tilde{\varepsilon}_n = \varepsilon_n + \Gamma_N \tilde{\varepsilon}_n \sqrt{\tilde{\varepsilon}_n^2 + \Delta^2}/\tilde{\varepsilon}_n, \tag{13}$$

with $\varepsilon_n = (2n+1)\pi T$. In the HSM model the gap and excitation spectrum are determined by the mean-free path l. Pair breaking occurs homogeneously throughout the liquid. The dimensionless pair-breaking parameter that determines T_c is given by the ratio $x_c = \Gamma_N/2\pi T_c$. At lower temperatures the pair-breaking parameter that enters the gap equation and renormalized Matsubara frequencies scales as $x = \Gamma_N/2\pi T$. Detailed discussion of the results for the magnetization within the HSM are given in Refs. 1 and 24.

When the inhomogeneities of the aerogel occur on length scales comparable to or greater than the pair correlation length, the HSM model overestimates the magnitude of pair breaking. For a fixed mean-free path this aerogel correlation effect leads to an increase in T_c, and to a reduction in the number of low-energy excitations produced by scattering within the aerogel. We introduce the effective pair-breaking parameter for the gap and excitation spectrum based on a similar scaling procedure introduced for the transition temperature.[7] For T_c the effective pair-breaking parameter, $\tilde{x}_c = x_c/(1+\zeta_a^2/x_c)$, interpolates between the HSM model with $\tilde{x}_c \propto -(\xi/l)$ valid for $\xi \gg \xi_a$ and the inhomogeneous limit with $\tilde{x}_c \propto -(\xi/\xi_a)^2$ valid for $\xi \ll \xi_a$. At lower temperatures the scaling is given by $\tilde{x} = x/(1+\zeta_a^2/x_c)$, which coincides with $\tilde{x}_c$ for $T \to T_c$, and accounts for the corresponding reduction in the pair-breaking density of states at temperatures $T \ll T_c$. Replacing the pair-breaking parameter of the HSM by the effective pair-breaking parameter leads to a modification of the

low-energy excitation spectrum and magnetization. Physical properties that are not spatially resolved on the scale of ξ_a should be well described by this approach.

The magnetization of superfluid ^{3}He in $\approx$98% aerogel was measured by NMR in pure ^{3}He in aerogel and with varying amounts of ^{4}He preplating, and for intermediate ($p=17.0$ bar) and high ($p=29.5$ bar) pressures. We use the analysis of the normal ^{3}He susceptibility (shown in Fig. 3) to subtract the solid ^{3}He component. In this pressure range the effects of inhomogeneity in the aerogel are clearly reflected in the weaker suppression of T_c compared to the relative suppression at lower pressures.[7] Figure 8 and shows results for the magnetic susceptibility of the "dirty" B phase calculated for a mean free path of $l=130$ nm. As is clearly shown T_c as predicted by the HSM model (i.e., $\xi_a=0$) is too strongly suppressed. In addition the HSM predicts a larger increase in the spin susceptibility for $T \to 0$, indicative of an overestimate of the density of polarizable low-energy quasiparticles.

The effect of aerogel correlations, corresponding to typical void sizes of $\xi_a \approx 40$–44 nm, is shown in both figures. The correlations lead to weaker suppression of T_c compared to the HSM model and to reduced pair breaking. Both effects are clearly seen in the data for both pressures, and are consistent with one another and with the mean-free path determined from the spin-diffusion data.

To summarize, we report on experimental measurements of the normal-state spin diffusion coefficient and magnetization of ^{3}He in 98% aerogel, with varying amounts of ^{3}He solid coating the aerogel strands. These results are compared with theoretical predictions for the spin-diffusion coefficient based on scattering from both the aerogel (elastic channel) and binary quasiparticle collisions (inelastic). The normal-state spin-diffusion measurements provide a determination of the elastic mean-free path $l=130$ nm for this porosity. The temperature dependence of the diffusion coefficient also agrees with the theory over the full temperature range, including the crossover regime, at both low and high pressures. Measurements of the nuclear magnetization in the superfluid phase of ^{3}He, in the same aerogel, show suppressions of the magnetization that are in quantitative agreement with a semi-

phenomenological theory of pair breaking based on quasiparticle scattering that includes correlation effects in the aerogel density, and the magnetic response of low-energy excitations in the "dirty" B phase of ^{3}He for this model for aerogel. A consistent interpretation of the data for the spin-diffusion coefficient, magnetization, and superfluid transition temperature is obtained when these aerogel correlation effects are included.

APPENDIX

The temperature dependence of the diffusion time for spin transport when both elastic and inelastic scattering channels are operative is obtained from an exact solution to the Landau-Boltzmann transport equation.[13] Details of this calculation are published separately.[14] Below we include the result for τ_D which we use to analyze the experimental data and to obtain the theoretical curves shown in Fig. 7

$$\tau_D = \frac{\tau_{in}}{4\pi^2} \sum_{N=0}^{even} \frac{1}{1 - \lambda_D/\alpha_N} \left\{ \sum_{l=0,2,\ldots}^{N} d_l \beta\left(\gamma + \frac{1}{2}; \frac{l+1}{2}\right) \right\}^2, \quad (A1)$$

where $\alpha_N = (\gamma+N)(1+2\gamma)+N(N-1)/2$, the Beta function, $\beta(\mu;\nu) = \Gamma(\mu)\Gamma(\nu)/\Gamma(\mu+\nu)$, is related to the standard Gamma function,[17] and

$$\gamma = \frac{1}{2}\sqrt{1 + \frac{1}{\pi^2}\frac{\tau_{in}}{\tau_{el}}} \quad (A2)$$

is the dimensionless parameter that controls the crossover from elastic- to inelastic-dominated scattering. The coefficients in Eq. (A1) are obtained from the recursion relation

$$d_{l+2} = \frac{l(l-1) + 2l(1+2\gamma) - 2\alpha_N + 2\gamma + 4\gamma^2}{(l+2)(l+1)} d_l \quad (A3)$$

and the normalization condition

$$1 = \sum_{l=0,2,\ldots}^{N} \sum_{l'=0,2,\ldots}^{N} d_l d_{l'} \left\{ 2\gamma^2 \beta\left(2\gamma; \frac{l+l'+1}{2}\right) \right.$$
$$+ 2\gamma^2 \beta\left(2\gamma; \frac{l+l'+3}{2}\right) - 2\gamma l' \beta\left(2\gamma+1; \frac{l+l'+1}{2}\right)$$
$$+ \left. \frac{1}{2}ll' \beta\left(2\gamma+2; \frac{l+l'-1}{2}\right) \right\}. \quad (A4)$$

[1] P. Sharma and J. A. Sauls, J. Low Temp. Phys. **125**, 115 (2001).

[2] P. Sharma, Ph.D. thesis, Northwestern University, 2003.

[3] E. Collin, Ph.D. thesis, Université Joseph Fourier, Grenoble, 2002.

[4] D. Rainer and J. A. Sauls, J. Low Temp. Phys. **110**, 525 (1998).

[5] E. V. Thuneberg, S.-K. Yip, M. Fogelström, and J. A. Sauls, Phys. Rev. Lett. **80**, 2861 (1998).

[6] G. Lawes, S. C. J. Kingsley, N. Mulders, and J. M. Parpia, Phys. Rev. Lett. **84**, 4148 (2000).

[7] J. A. Sauls and P. Sharma, Phys. Rev. B **68**, 224502 (2003).

[8] G. Gervais, K. Yawata, N. Mulders, and W. P. Halperin, Phys. Rev. B **66**, 054528 (2002).

[9] D. T. Sprague, T. M. Haard, J. B. Kycia, M. R. Rand, Y. Lee, P. J. Hamot, and W. P. Halperin, Phys. Rev. Lett. **75**, 661 (1995).

[10] C. Winkelmann, E. Collin, Y. M. Bunkov, and H. Godfrin, J. Low Temp. Phys. **135**, 3 (2004).

[11] H. Godfrin and R. E. Rapp, Adv. Phys. **44**, 113 (1995).

[12] A. Golov and F. Pobell, Phys. Rev. B **53**, 12 647 (1996).

[13] P. Sharma and J. A. Sauls, Physica B **284–288**, 297 (2000).

[14] P. Sharma and J. A. Sauls (unpublished).

[15] G. A. Brooker and J. Sykes, Phys. Rev. Lett. **21**, 279 (1968).

[16] G. Baym and C. J. Pethick, *Landau Fermi-Liquid Theory* (Wiley, New York, 1991).

[17] M. Abramowitz and I. A. Stegun, *Handbook of Mathematical Functions* (Dover, New York, 1970).

[18] A. C. Anderson, W. Reese, and J. C. Wheatley, Phys. Rev. **127**, 671 (1962).

[19] J. A. Sauls and J. W. Serene, Phys. Rev. B **24**, 183 (1981).

[20] W. P. Halperin and E. Varoquaux, in *Helium Three*, edited by W. P. Halperin and L. P. Pitaevskii (Elsevier Science, Amsterdam, 1990), p. 353.

[21] D. Candela and N. Kalechofsky, J. Low Temp. Phys. **113**, 351 (1998).

[22] B. I. Barker, Y. Lee, L. Polukhina, D. D. Osheroff, L. W. Hrubesh, and J. F. Poco, Phys. Rev. Lett. **85**, 2148 (2000).

[23] J. W. Serene and D. Rainer, Phys. Rep. **101**, 221 (1983).

[24] V. P. Mineev and P. L. Krotkov, Phys. Rev. B **65**, 024501 (2002).